Sustainable Food Technology

ROYAL SOCIETY OF CHEMISTRY

PAPER

View Article Online
View Journal

Cite this: DOI: 10.1039/d6fb00124f

Optimization of spray-dried green tea polyphenol microcapsules using a yeast-derived polysaccharide-rich fraction: encapsulation performance, structural characterization, and controlled release behavior

Hien Thi Do [ab] and Tuyen Chan Kha [*a]

Polyphenols are highly susceptible to oxidative, thermal, and photodegradation, limiting their functional efficacy in food systems. This study developed a sustainable microencapsulation approach using a yeast-derived polysaccharide-rich fraction from brewer's spent yeast, combined with maltodextrin, to enhance polyphenol stability. Spray-drying conditions were optimized *via* a Box–Behnken design, yielding high encapsulation efficiency (90.49%) and yield (41.80 mg g^{-1}) under optimal parameters (0.44 w w^{-1}, 143 °C, and 5.3 mL min^{-1}; R^2 > 0.96). Structural analyses (SEM and FTIR) confirmed successful encapsulation and a typical particle morphology. Encapsulation markedly improved resistance to thermal, oxidative, and photodegradation compared to free extracts. Release studies in simulated food and gastrointestinal systems revealed matrix-dependent behavior, with maltodextrin–soy protein systems showing rapid release (~80%) and maltodextrin–polysaccharide systems enabling sustained release (~50–55%). Encapsulated polyphenols retained bioactivity during digestion. Overall, the yeast-derived polysaccharide-rich fraction represents a sustainable and effective wall material for high-efficiency microencapsulation and controlled delivery in functional food applications.

Received 14th April 2026
Accepted 27th April 2026

DOI: 10.1039/d6fb00124f

rsc.li/susfoodtech

Sustainability spotlight

This study presents a sustainable bioprocessing strategy that valorises brewer's spent yeast as a functional encapsulating material for polyphenol delivery. Yeast-derived polysaccharides, rich in β-glucan and mannoproteins, were integrated into a spray-drying system, reducing reliance on conventional carriers and supporting circular bioeconomy principles. Process optimisation *via* response surface methodology enhanced the encapsulation efficiency while minimising resource use. The resulting microcapsules significantly improved polyphenol stability against thermal, photochemical, and oxidative degradation and enabled controlled release under simulated food and gastrointestinal conditions. By converting low-value brewing by-products into high-value ingredients, this work advances resource efficiency and sustainable innovation, providing a scalable framework for eco-efficient functional food development aligned with SDGs 3, 9, 12, and 13.

1 Introduction

Polyphenols are bioactive phytochemicals widely recognized for their antioxidant, anti-inflammatory, and cardiometabolic protective effects. However, their incorporation into food systems remains technically challenging because of their pronounced sensitivity to oxygen, light, heat, and pH variations.[1] From a reaction engineering perspective, polyphenol degradation is governed by oxygen diffusion, moisture-mediated hydrolysis, and temperature-dependent oxidation kinetics, leading to rapid loss of bioactivity during processing, storage, and digestion.[2] Consequently, effective stabilization strategies are required to preserve the structural integrity and functional performance of polyphenols in food applications.

Microencapsulation is a well-established approach to enhance the stability, handling properties, and controlled delivery of sensitive bioactives. Among the available encapsulation techniques, spray drying remains one of the most industrially scalable and cost-effective technologies due to its operational simplicity, continuous processing capability, compatibility with heat-sensitive compounds, and adaptability to food-grade materials when properly optimized. Nevertheless, the success of spray-drying microencapsulation depends highly on both the physicochemical characteristics of the wall material and the control of process parameters. Spray-drying variables such as core-to-wall ratio, inlet temperature, feed flow rate and

[a]Faculty of Chemical Engineering and Food Technology, Nong Lam University, Ho Chi Minh City 700000, Vietnam. E-mail: khachantuyen@hcmuaf.edu.vn
[b]Faculty of Biology and Environment, Ho Chi Minh City University of Industry and Trade, Ho Chi Minh City 700000, Vietnam

feed concentration directly influence droplet evaporation, crust formation, internal porosity, and residual moisture, thereby determining the encapsulation efficiency, powder recovery, particle morphology, matrix integrity, and release behavior.

Although release occurs at the final stage of encapsulation, it must be considered during system design because it ultimately determines functional performance. The rate and mechanism of release are strongly influenced by both the wall material characteristics and the encapsulation method. Well-controlled release is a defining property of effective microcapsules, particularly when targeted or time-dependent delivery is desired.[3] Therefore, elucidating how structural features formed during spray drying influence release behavior is critical for rational formulation development.

The release kinetics of spray-dried systems are commonly described using diffusion-based models. In structurally stable matrices, transport typically follows Fickian diffusion, driven by concentration gradients. In contrast, hydrophilic biopolymer systems capable of swelling or structural relaxation often exhibit anomalous (non-Fickian) diffusion, in which solvent penetration induces polymer relaxation and coupled diffusion–relaxation transport mechanisms.[4] The dominance of diffusion or relaxation processes depends strongly on matrix composition, hydrogen bonding interactions, and environmental conditions. Consequently, understanding structure–transport relationships is essential for rational system design.

The selection of wall material is particularly important for controlling both encapsulation performance and release behavior. Maltodextrin (MD) is widely used in spray drying due to its high solubility, low viscosity, and good drying properties. However, its highly hydrophilic nature may lead to rapid hydration, porous matrix formation, and fast diffusion of encapsulated compounds. Protein-based carriers such as soy protein isolate (SPI) may enhance film formation and interfacial stabilization, but they may undergo conformational changes under thermal processing or enzymatic digestion, thereby affecting matrix integrity. In this context, a yeast-derived polysaccharides-rich fraction obtained from brewer's spent yeast represents a promising alternative wall material. Brewer's spent yeast is an abundant by-product of beer production that remains underutilized, with a substantial fraction being discharged as waste. Yeast cell walls constitute approximately 20–30% of dry biomass and are primarily composed of β-glucan (50–60%), mannoproteins (30–40%), and minor amounts of chitin.[5,6] These structural biopolymers may contribute to the formation of cohesion matrices with improved barrier properties and release-modulating capacity.

From a mechanistic perspective, the yeast-derived polysaccharide-rich fraction may interact with polyphenols through several complementary mechanisms. The abundance of hydroxyl groups in both polysaccharides and polyphenols favors hydrogen bonding,[7] while hydrophobic interactions may occur between the aromatic rings of polyphenols and less polar regions of the carrier matrix.[8] In addition, the β-glucan-rich three-dimensional network can physically entrap bioactive compounds, increase diffusional tortuosity, and reduce oxygen penetration. These structural features may contribute to improved retention of polyphenols during spray drying and storage, as well as more sustained release under simulated food and gastrointestinal conditions.[9]

Recent studies have highlighted the potential of yeast-derived cell-wall materials and β-glucan-based systems as functional carriers for sensitive bioactive compounds. Yeast cell-wall polysaccharides have been suggested to form semi-permeable matrices that may restrict oxygen diffusion and improve the stability of encapsulated polyphenols during spray drying and storage.[10] β-Glucan-rich systems have also been explored as delivery matrices because of their hydration, swelling, and interaction with aqueous and gastrointestinal environments, which may contribute to controlled release behavior.[11,12] In addition, plasmolyzed *Saccharomyces cerevisiae* cells have been reported as effective microencapsulation materials for plant polyphenols, with high encapsulation efficiency and enhanced antioxidant stability.[13] Yeast-derived matrices have also been applied to encapsulate and stabilize other bioactive compounds, including resveratrol,[2] fish oil,[14] and D-limonene.[15] Moreover, several studies have emphasized the influence of carrier composition and environmental conditions on the release kinetics of polyphenol systems.[16–18] These findings suggest that brewer's spent yeast-derived polysaccharide-rich fractions may serve not only as sustainable wall materials but also as functional matrices capable of improving bioactive protection and release modulation.

Despite these advances, the systematic optimization of spray-drying conditions for polyphenol microencapsulation using yeast-derived polysaccharide-rich fractions remains insufficiently explored. In particular, limited information is available on how process variables influence encapsulation performance, particle structure, environmental stability, and release behavior within an integrated process–structure–function framework. Although previous work demonstrated the feasibility of employing yeast-derived polysaccharides as a carrier matrix for polyphenol encapsulation,[19] the effects of spray-drying parameters on matrix formation, stability, and controlled-release behavior were not fully elucidated.

Therefore, the present study aimed to optimize the spray-drying conditions for producing green tea polyphenol microcapsules using maltodextrin combined with a yeast-derived polysaccharide-rich fraction obtained from brewer's spent yeast. A Box–Behnken response surface design was applied to evaluate the effects of core-to-wall ratio, inlet temperature, and feed flow rate on the encapsulation yield and encapsulation efficiency. The optimized powders were further characterized in terms of morphology, functional groups, and thermal, photochemical, and oxidative stability, as well as release behavior in simulated food and gastrointestinal media. The novelty of this study is the development of a sustainable spray-dried polyphenol delivery system that valorizes brewer's spent yeast while establishing a process–structure–function relationship between spray-drying conditions, wall-matrix characteristics, polyphenol protection, and release modulation. This study provides a mechanistic basis for the development of sustainable biopolymer-based delivery systems for functional food applications.

2 Materials and methods

2.1 Chemicals and wall materials

Folin–Ciocalteu reagents and DPPH (2,2-diphenyl-1-picrylhydrazyl) were purchased from Sigma-Aldrich. The protease (2.5 AU-A per g, optimal pH 5.5) utilized in this study was supplied by Novozymes. All chemicals and reagents used for antioxidant assays and simulated digestion media were of analytical grade. Maltodextrin (MD, DE 10–12, France) and soy protein isolate (SPI, protein content ≥90%, dry basis, USA) were used as wall materials.

2.2 Preparation of raw materials

2.2.1 Preparation and characterization of the yeast-derived polysaccharide-rich fraction. The yeast-derived polysaccharide-rich fraction (PS) was prepared from brewer's spent yeast according to the method described in our previous study,[19] with slight modifications. Fresh brewer's spent yeast slurry obtained from Sai Gon Brewery (Binh Tan, Ho Chi Minh City, Vietnam) was mixed with sterile water at a yeast-to-water ratio of 1 : 3 (w v^{-1}). The suspension was then allowed to settle for 1 h. Thereafter, the upper and lower layers of sediment were removed, leaving the remaining liquid portion. The washing procedure was repeated thrice. Subsequently, the yeast biomass was amalgamated with a 0.5% (w v^{-1}) NaCl solution at a ratio of 1 : 3 (w v^{-1}), allowed to settle for 1 h, and the supernatant was removed. The remaining biomass was centrifuged at 4500 rpm for 15 min to obtain purified yeast cells. The biomass was stored at −20 °C until further use.

For extraction, 10 g of yeast biomass was treated with 3% (w v^{-1}) protease and incubated at 45 °C for 6 h. Subsequently, 40 mL of distilled water was added, and the mixture was sonicated for 10 min. The suspension was centrifuged at 4500 rpm for 15 min, and the precipitate was collected. The residue was washed thrice with distilled water and centrifuged to obtain the yeast-derived polysaccharide-rich fraction.[19]

The obtained fraction was characterized as a polysaccharide-rich yeast cell wall material. Based on compositional analysis of the tested fraction, the material contained 59.5% total polysaccharides, 9.01% protein, and 5.57% β-glucan on an as-received basis. The residual protein fraction was retained in the material and is noteworthy because it may contribute to matrix formation and polyphenol–carrier interactions during spray-drying microencapsulation.

2.2.2 Polyphenol extraction. Green tea leaves were procured from Lam Ha District, Lam Dong Province, Vietnam. The leaves were dried at 60 °C to a final moisture content of approximately 5% and ground into powder. Polyphenols were extracted as described by Friedman *et al.*,[20] with slight modifications. Briefly, tea powder was extracted with 80% (v v^{-1}) ethanol at a solid-to-solvent ratio of 1 : 10 (w v^{-1}) at 80 °C for 30 min. The extract was then centrifuged at 4500 rpm for 10 min, and the supernatant was concentrated under reduced pressure using a rotary evaporator until a concentrated extract with a moisture content of approximately 20% was obtained. The total phenolic content of the extract was 327.974 mg gallic acid equivalents per gram of dry matter. Therefore, the extract was described as a green tea polyphenol-rich extract rather than a purified polyphenol fraction. The concentrated extract, designated as the core material, was stored under refrigeration until its subsequent use in experiments.

2.3 Optimization and stability assessment of spray-dried polyphenol powder

2.3.1 Optimization. The spray-drying conditions were optimized using a Box–Behnken response surface design (JMP 13.0) to maximize the encapsulation yield (Y_1, mg g^{-1}) and encapsulation efficiency (Y_2, %). The independent variables were the core-to-wall ratio (X_1: 0.3–0.5 w w^{-1}), the inlet air temperature (X_2: 130–150 °C), and the feed flow rate (X_3: 4–6 mL min^{-1}). A three-factor, three-level Box–Behnken design (BBD) was employed to evaluate the effects of process variables on encapsulation performance. The experimental data were then fitted to a second-order polynomial regression model:

$$Y = \beta_0 + \sum \beta_i X_i + \sum \beta_{ii} X_i^2 + \sum \beta_{ij} X_i X_j$$

Where Y represents the response variable, which is denoted as the encapsulation yield or encapsulation efficiency; β_0 is the intercept; β_i, β_{ii}, and β_{ij} are linear, quadratic, and interaction coefficients, respectively; X_i and X_j are coded as independent variables.

To optimize the microencapsulation of polyphenols, the concentrated extract was incorporated into a wall material solution composed of yeast-derived polysaccharide and maltodextrin at a fixed ratio of 10 : 1 (w w^{-1}), according to the experimental design. The total solid content of the feed solution was adjusted to approximately 20% (w w^{-1}). The mixture was homogenized using an IKA RW 20 homogenizer (Germany) at 4200 rpm for 15 min to ensure uniform dispersion and subsequently spray-dried using a LabPlant SD-06 spray dryer (UK) under the designated inlet temperature and feed flow rate conditions (atomizing air pressure of 1 bar). The obtained powders were vacuum-sealed and stored at 4 °C until further analysis.

The adequacy of the model was evaluated using the coefficient of determination (R^2), the adjusted R^2, the lack-of-fit test, and the analysis of variance (ANOVA). The optimization process was performed using a desirability function methodology to maximize both the encapsulation yield and encapsulation efficiency. The surface morphology of the optimal spray-dried powders was examined by scanning electron microscopy (SEM), and functional group analysis was done by Fourier-transform infrared (FTIR) spectroscopy.

2.3.2 Stability assessment. The evaluation of oxidative stability was conducted by storing 1 g samples (under vacuum and non-vacuum conditions) at ambient temperature in the absence of light. The total polyphenol content (TPC) and DPPH radical scavenging activity of these samples were then measured after 3, 6, and 9 days.[21]

Photostability was assessed under 10 000, 22 000, and 34 000 Lux, while thermal stability was examined at 70, 80, 90, and

100 °C for 1–3 h. The TPC and antioxidant activity were determined at designated intervals.[21]

2.4 Release study

To evaluate the effect of wall material composition on polyphenol release behavior, the optimized spray-dried microcapsules were compared with two reference wall systems, namely MD and MD + SPI. The MD and MD + SPI formulations were prepared under fixed spray-drying conditions adapted from our previous study,[19] with minor modifications to ensure stable powder production and comparability among the reference systems. Briefly, 70 g of concentrated green tea polyphenol-rich extract was dispersed in 200 mL of distilled water. Subsequently, either 240 g of MD or a mixture of 150 g MD and 90 g SPI was added under magnetic stirring. The volume was adjusted to 1500 mL with distilled water, followed by homogenization at 4200 rpm for 15 min. The resulting feed mixtures were spray-dried at an inlet air temperature of 150 °C, a feed rate of 5 mL min^{-1}, and a compressed air pressure of 1 bar. The outlet air temperature ranged from 73 to 80 °C during drying.

Response surface optimization was conducted only for the MD + PS formulation, as the main objective of this study was to assess the role of the yeast-derived polysaccharide-rich fraction as a functional wall material. The MD and MD + SPI formulations were used solely as reference systems and were therefore not independently optimized. This design enabled the comparison of release behavior mainly as a function of wall material composition.

2.4.1 Release in simulated food media. Encapsulated powders (MD, MD + SPI, and MD + PS systems) were produced by spray drying as described above. The release of polyphenols was evaluated in model food media containing 10%, 20%, and 50% (v v^{-1}) ethanol and 3% (v v^{-1}) acetic acid. Briefly, 0.2 g of powder was dispersed in 20 mL of the respective medium, vortexed for 30 s, and subsequently analyzed for released polyphenols after 5, 30, 60 and 120 min according to the method described by Talón *et al.*[22]

2.4.2 Release in simulated gastrointestinal fluids. The simulated gastric fluid (SGF, pH 1.2, pepsin-containing) and simulated intestinal fluid (SIF, pH 6.8, pancreatin-containing) were prepared according to the procedure previously described by Dag *et al.*[23] Samples (0.2 g) were incubated in 20 mL SGF or SIF at 37 °C with shaking. Aliquots were withdrawn at 5, 30, 60, and 120 min, and the enzyme activity was terminated by pH adjustment.[18] The amount of released polyphenols was then quantified using the Folin–Ciocalteu method.

2.5 Analyses

2.5.1 Total polyphenol content. Total polyphenol content (TPC) was determined using the Folin–Ciocalteu colorimetric method,[24] with gallic acid as the calibration standard. A gallic acid stock solution (4000 μg mL^{-1}) was prepared by dissolving 0.004 g in 1 mL distilled water and subsequently diluted to 10–100 μg mL^{-1} for the standard curve. For calibration, 0.5 mL of standard solution was mixed with 0.5 mL Folin–Ciocalteu reagent and incubated for 5 min. Then, 4 mL of 2% (w v^{-1}) Na_2CO_3 was added, and the mixture was incubated at room temperature for 20 min before measuring absorbance at 765 nm using a UV–vis spectrophotometer (7305, Cole-Parmer, Jenway, UK).

For encapsulated powders, phenolic compounds were extracted using methanol : acetic acid : water (50 : 8 : 42, v : v : v) to promote matrix swelling and disruption and to weaken interactions between the wall materials and entrapped polyphenols. Spray-dried powder samples (200 mg) were mixed with 2 mL of the extraction solvent, vortexed for 1 min, ultrasonicated for 20 min, and centrifuged at 5000 rpm for 5 min. The resulting supernatant was collected and analyzed using the Folin–Ciocalteu procedure described above.

For the concentrated green tea extract, the sample was dispersed in distilled water because the phenolic compounds were present in a non-encapsulated and readily soluble form. Briefly, 0.004 g of the concentrated extract was dissolved in 1 mL of distilled water and treated under the same Folin–Ciocalteu reaction conditions. The calibration standard, reaction time, and absorbance measurement conditions were kept consistent for all samples. Therefore, the obtained values were reported as recoverable total phenolic content under the specified extraction conditions.

TPC was expressed as mg gallic acid equivalents per gram of dry weight (mg GAE g^{-1} DW) and calculated as:

$$\mathrm{TPC} = \frac{X \times V \times f}{m}$$

where X is the concentration determined from the standard curve (μg mL^{-1}), V is the volume of the sample (mL), f is the dilution factor, and m is the sample mass (g).

2.5.2 Antioxidant activity. Antioxidant activity was determined using the DPPH radical scavenging assay. For spray-dried powder samples, 0.2 g of sample was accurately weighed and dissolved in 4 mL of buffer solution (methanol : acetic acid : water, 50 : 8 : 42, v : v : v). The mixture was vortexed for 1 min, followed by ultrasonication for 20 min. The suspension was then centrifuged at 4500 rpm for 10 min. Subsequently, 2 mL of the supernatant (diluted 1000-fold) was mixed with 2 mL of DPPH solution and incubated in the dark at room temperature for 30 min. The absorbance was measured at 517 nm. The DPPH solution was prepared in methanol at a concentration of 40 μg mL^{-1} according to the method described by Lu and Chen.[21]

For the non-encapsulated green tea polyphenol-rich extract, 0.2 g of the extract was weighed and dissolved in 4 mL of methanol, followed by a 1000-fold dilution. An aliquot of 2 mL of the diluted solution was mixed with 2 mL of DPPH solution and treated under the same conditions as described above.

The antioxidant activity, expressed as the percentage of DPPH radical scavenging activity, was calculated using the following equation:

$$I\ (\%) = 100 \times \frac{A_o - A_1}{A_o}$$

where I (%) represents the percentage of DPPH radical scavenging activity at 517 nm; A_o is the absorbance of the DPPH control; A_1 is the absorbance of the sample solution.

The obtained values were expressed as the apparent radical-scavenging activity of the recovered phenolic fraction under the specified extraction and dilution conditions. Total phenolic content was determined in parallel to support the interpretation of antioxidant retention.

2.5.3 Encapsulation yield (EY). The encapsulation yield was calculated as follows:

$$EY\ (\mathrm{mg\ g^{-1}}) = \frac{\text{The amount of encapsulated polyphenols}}{\text{Mass of recovered powder}} \times 100$$

2.5.4 Encapsulation efficiency (EE). Surface polyphenols were extracted by washing with ethanol,[25] and total polyphenols were determined after complete dissolution of the microcapsules.

$$\mathrm{EE}\ (\%) = \frac{\text{Total polyphenols} - \text{Surface polyphenols}}{\text{Total polyphenols}} \times 100$$

The TPC was quantified using the Folin–Ciocalteu method and expressed as gallic acid equivalents.[24]

2.5.5 Surface morphology. The surface morphology of the spray-dried powder was examined using a SEM (JSM 7401F, JEOL, Tokyo, Japan), with an acceleration voltage of 10–30 kV. Representative SEM images were captured at different magnifications of 1000×, 2000×, and 5000×.

2.5.6 FTIR spectroscopy. The chemical functionalities of the spray-dried powder were characterized using FTIR spectroscopy with a Bruker Tensor 37 instrument (USA). Infrared spectra were collected within the wavenumber interval of 400–4000 $\mathrm{cm^{-1}}$ at a spectral resolution of 4 $\mathrm{cm^{-1}}$, averaging 32 scans for each sample. The acquired spectra were subsequently interpreted to elucidate the possible molecular interactions between the encapsulated bioactive constituents and the surrounding wall matrix.

2.5.7 Determination of polyphenol release. The concentration of released polyphenols was quantified using the Folin–Ciocalteu method. Briefly, 0.5 mL of the appropriately treated sample solution collected at each experimental condition and time point was transferred into a test tube and analyzed as described previously.[26]

For encapsulated samples,[27] the percentage of polyphenol release was calculated as follows:

$$\mathrm{Release}\ (\%) = \frac{\text{Polyphenols released at sampling time} - \text{Surface polyphenols}}{\text{Total encapsulated polyphenols}} \times 100$$

For non-encapsulated (free extract) samples,[27] release was calculated as:

$$\mathrm{Release}\ (\%) = \frac{\text{Polyphenols released at sampling time}}{\text{Total polyphenols in the extract}} \times 100$$

2.6 Statistical analysis

All experiments were conducted in triplicate, and results are expressed as mean ± standard deviation. Data were processed using Microsoft Excel 2010 and statistically analyzed using Statgraphics Centurion XVI. Optimization of spray-drying conditions was performed using JMP version 13.0. Differences were considered statistically significant at the 95% confidence level ($p < 0.05$).

3 Results and discussion

3.1 Process optimization

3.1.1 Model fitting and statistical adequacy. As shown in Tables 1 and 2, the encapsulation yield ranged from 30.04 to 41.22 mg $\mathrm{g^{-1}}$, with the highest value observed at the central experimental point ($X_1 = 0.4$; $X_2 = 140$ °C; $X_3 = 5$ mL $\mathrm{min^{-1}}$). The quadratic model was statistically significant ($R^2 = 0.96$; $p < 0.01$), indicating strong explanatory power. The significant terms ($p < 0.05$) included the linear effects of the core-to-wall ratio (X_1) and inlet temperature (X_2), the interaction between the core-to-wall ratio and the feed flow rate (X_3), and the quadratic terms of all three variables. The fitted second-order regression equation for the EY (Y_1) is as follows:

$$Y_1 = 40.65 + 2.99X_1 + 1.37X_2 + 1.92X_1X_3 - 3.10{X_1}^2 - 2.43{X_2}^2 - 4.18{X_3}^2$$

The encapsulation efficiency varied from 69.76 to 90.24%, with the maximum obtained in experimental run 9. The regression model exhibited excellent predictability ($R^2 = 0.99$; $p < 0.001$). Significant effects were associated primarily with the linear and quadratic terms of core-to-wall ratio and feed flow rate, as well as their interaction (Tables 1 and 2). The regression equation for EE (Y_2) is as follows:

$$Y_2 = 89.42 + 5.05X_1 + 2.19X_3 + 1.74X_1X_3 + 1.52X_2X_3 - 7.86{X_1}^2 - 3.56{X_2}^2 - 6.21{X_3}^2$$

The findings are supported by the consistently high coefficients of determination ($R^2 > 0.95$) and non-significant lack-of-fit, which confirm that the quadratic models adequately captured nonlinear interactions among drying variables and reliably predicted the encapsulation performance. Beyond statistical validation, the observed response patterns can be mechanistically interpreted through the coupled effects of heat transfer, solvent evaporation, droplet shrinkage, and matrix consolidation during spray drying.[28] The balance among these phenomena governs both polyphenol retention and powder recovery.

Table 1 Effects of process variables on the encapsulation yield (EY) and encapsulation efficiency (EE)[a]

Exp.	Code	Core-to-wall ratio, X_1 (w w^{-1})	Inlet temperature, X_2 (°C)	Feed flow rate, X_3 (mL min^{-1})	EY (mg g^{-1})	EE (%)
1	−−0	0.3	130	5	31.72	71.37
2	−0−	0.3	140	4	30.62	69.76
3	−0+	0.3	140	6	30.04	71.69
4	−+0	0.3	150	5	32.64	73.61
5	0−−	0.4	130	4	31.55	78.99
6	0−+	0.4	130	6	31.92	79.31
7	000	0.4	140	5	41.22	89.53
8	000	0.4	140	5	40.45	88.48
9	000	0.4	140	5	40.30	90.24
10	0+−	0.4	150	4	35.09	76.93
11	0++	0.4	150	6	37.60	83.33
12	+−0	0.5	130	5	37.66	82.77
13	+0−	0.5	140	4	32.87	75.50
14	+0+	0.5	140	6	39.96	84.39
15	++0	0.5	150	5	38.46	84.23

[a] (+) Upper value; (−) lower value; (0) value at midpoint.

Table 2 Statistical significance of model terms for the encapsulation yield and encapsulation efficiency[a]

	Encapsulation yield (EY)		Encapsulation efficiency (EE)	
Term	t ratio	Prob > $\|t\|$	t ratio	Prob > $\|t\|$
β_0	51.95	<0.0001[b]	145.70	<0.0001[b]
X_1	6.24	0.0015[b]	13.46	<0.0001[b]
X_2	2.85	0.0357[b]	1.88	0.1185
X_3	2.45	0.0580	5.83	0.0021[b]
$X_1 \times X_2$	−0.04	0.9664	−0.37	0.7287
$X_1 \times X_3$	2.83	0.0367[b]	3.27	0.0221[b]
$X_2 \times X_3$	0.79	0.4657	2.86	0.0354[b]
$X_1 \times X_1$	−4.40	0.0070[b]	−14.21	<0.0001[b]
$X_2 \times X_2$	−3.45	0.0182[b]	−6.43	0.0013[b]
$X_3 \times X_3$	−5.93	0.0019[b]	−11.24	<0.0001[b]

[a] β_0: intercept; X_1: core-to-wall ratio (w w^{-1}); X_2: inlet temperature (°C); X_3: feed flow rate (mL min^{-1}). [b] Statistically significant at $p < 0.05$.

3.1.2 Effect of core-to-wall ratio. The core-to-wall ratio had the most pronounced influence on both the EY and EE. At 0.3 w w^{-1}, the encapsulation performance was found to be constrained, with the EE ranging from 69.76% to 73.61% and the EY ranging from 30.04 mg g^{-1} to 32.64 mg g^{-1}. The presence of excess wall material led to a dilution of the polyphenol concentration per gram of powder. This, in turn, resulted in a reduction in the apparent yield and an increase in the relative diffusivity of solutes toward the surface. Moreover, a disproportionate polymer content may increase the feed viscosity, thus affecting the atomization uniformity.

At 0.4 w w^{-1}, both the EY and EE increased markedly (EE up to 90.24%; EY up to 41.22 mg g^{-1}), suggesting sufficient polymer coverage to form a continuous protective matrix around polyphenol-laden droplets. This ratio likely enhanced matrix continuity, increased path tortuosity, and reduced effective diffusivity within the droplet during drying.

When the ratio increased to 0.5 w w^{-1}, encapsulation performance declined (EE: 75.50–84.39%). Excessive core loading may have decreased the effective wall thickness per unit core mass, reducing the mass transfer resistance required to maintain solute entrapment. Additionally, the hygroscopic nature of tea polyphenols likely increased powder stickiness, leading to wall deposition within the drying chamber and reduced recovery.

The incorporation of MD in conjunction with PS has been shown to enhance the drying efficiency by increasing total solids and reducing adhesiveness, thereby facilitating powder recovery. As noted by Quek *et al.*,[29] MD modifies the surface adhesion properties of low-molecular-weight sugars and organic acids, thereby enhancing the drying efficiency and reducing the residual moisture.

3.1.3 Effect of inlet temperature. The impact of inlet temperature on matrix formation and polyphenol stability is a subject of significant interest. Increasing temperature has been shown to enhance heat transfer and accelerate moisture evaporation, promoting rapid crust formation around droplets.[30] The process of rapid evaporation contributes to surface solidification that occurs prior to solute back-diffusion, thereby increasing the encapsulation efficiency.

However, excessively high temperatures (150 °C) may induce structural stress and thermal degradation of polyphenols. In contrast, lower temperatures (130 °C) result in higher residual moisture, particle agglomeration, and adhesion to dryer walls, reducing the recovery efficiency.[29] The intermediate temperature range (approximately 140–143 °C) was found to provide an optimal balance between solvent removal and structural integrity.

3.1.4 Effect of feed flow rate. As reported by Devakate *et al.*,[31] the feed flow rate influences not only the droplet size distribution but also the residence time within the drying chamber. These parameters directly influence the heat and mass transfer dynamics during spray drying and, consequently, the structural development of microcapsules.

At lower feed flow rates, atomization generally produces smaller droplets with higher surface-to-volume ratios. This condition facilitates rapid solvent evaporation and earlier surface solidification. However, excessively low feed rates may extend the effective thermal exposure time of droplets within the drying chamber, increasing the likelihood of thermal stress

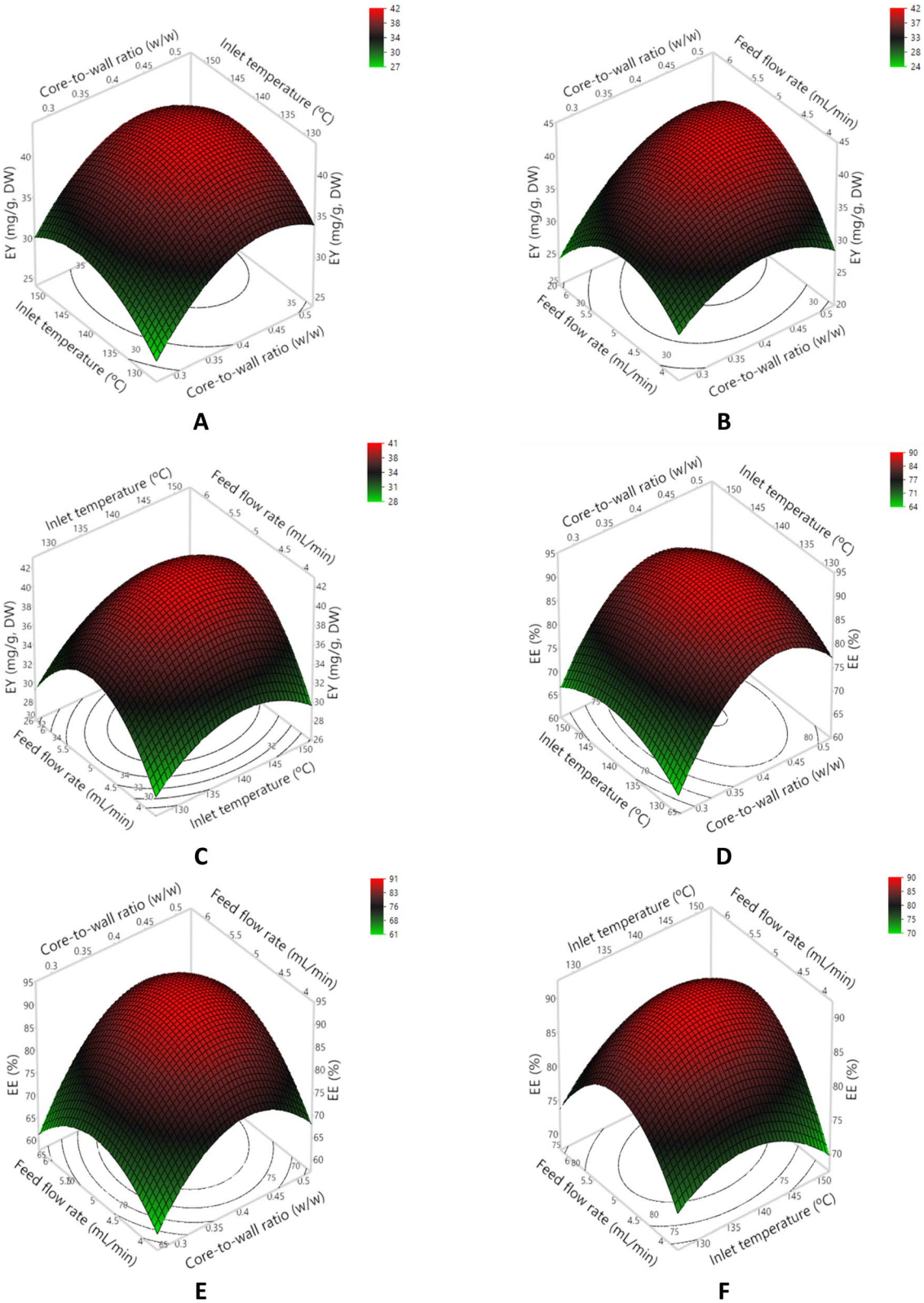

Fig. 1 Response surface plots illustrating the effects of process variables on the encapsulation yield (A–C) and encapsulation efficiency (D–F).

and degradation of heat-sensitive polyphenols. Conversely, higher feed flow rates tend to generate larger droplets and shorten the effective residence time. Under such conditions, solvent removal may be incomplete, leading to elevated residual moisture and delayed matrix consolidation. Insufficient structural strengthening during drying can compromise particle integrity and reduce encapsulation performance. Similar observations regarding the impact of residence time and drying completeness on structural stability have been reported.[32]

The statistically significant quadratic effect of X_3 (Table 2) confirms that the relationship between the feed flow rate and encapsulation responses is non-linear, indicating the presence of an optimal operating region rather than a monotonic trend. In the present study, an intermediate feed flow rate of approximately 5–5.3 mL min^{-1} provided a balanced drying regime, ensuring adequate solvent removal and matrix formation without inducing excessive thermal or structural stress. This condition contributed to maximizing the encapsulation efficiency while maintaining high powder recovery.

3.1.5 Response surface visualization and optimization. As illustrated in Fig. 1, the three-dimensional response surface plots reveal pronounced nonlinear interactions among the investigated variables. Numerical optimization identified the optimal spray drying conditions as a core-to-wall ratio of 0.44 (w w^{-1}), an inlet temperature of 143 °C, and a feed flow rate of 5.3 mL min^{-1} (Fig. 2). Under these conditions, the model predicted an encapsulation yield (EY) of 41.80 mg g^{-1} and an encapsulation efficiency (EE) of 90.49%. Experimental validation produced values of 41.40 mg g^{-1} for the EY and 90.08% for the EE (Table 3), demonstrating excellent agreement with the predicted responses and confirming the adequacy and predictive robustness of the regression models.

Notably, compared with our previous experimental conditions,[19] optimization in the present design resulted in a substantial improvement in performance, with the EY increasing by 24.8% and the EE by 3.7%. These gains underscore the effectiveness of response surface methodology in identifying synergistic parameter combinations that enhance both polyphenol retention and powder recovery.

Table 3 Predicted and experimental values of the optimum experimental conditions

Parameters	Predicted value	Experimental value
Core-to-wall material ratio (w w^{-1})	0.44	0.44
Inlet temperature (°C)	143	143
Feed flow rate (mL min^{-1})	5.3	5.3
Encapsulation yield (mg g^{-1})	41.80	41.40
Encapsulation efficiency (%)	90.49	90.08

In comparison with the findings of previous studies, the encapsulation efficiency obtained in this study exceeded the values reported for polyphenol encapsulation using gum arabic and maltodextrin.[25,33] This improvement suggests that the incorporation of yeast-derived polysaccharides contributes to enhanced matrix formation, structural cohesion, and retention capacity during spray drying.

Several studies have demonstrated that yeast-derived polysaccharide systems can form stable microcapsules through spray drying, thereby improving the encapsulation efficiency and providing effective protection for sensitive compounds, such as carotenoids[34] and polyphenols,[19] under thermal and oxidative conditions. Compared with conventional wall materials, including maltodextrin, gum arabic, and milk proteins, yeast polysaccharides may offer enhanced functional performance owing to their β-glucan-rich three-dimensional network structure, which facilitates interactions with polyphenols through hydrogen bonding and hydrophobic interactions.[35] These molecular

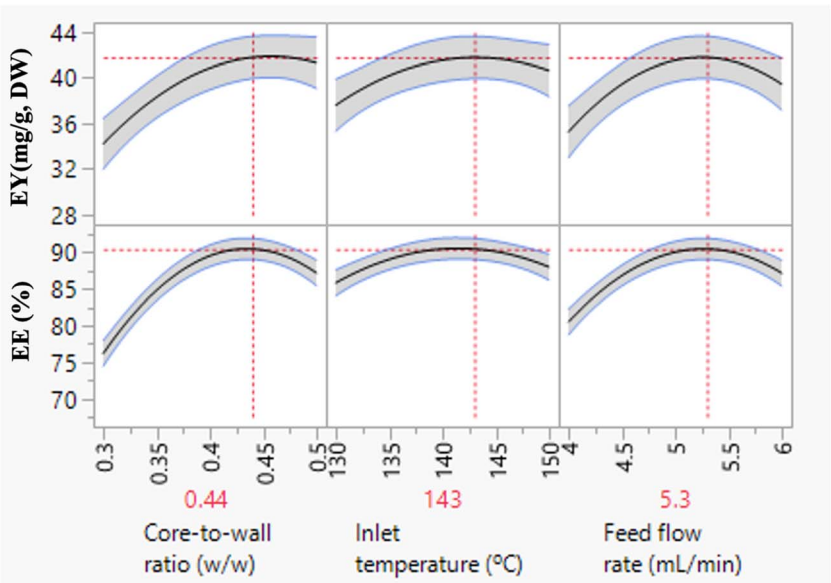

Fig. 2 Prediction profiler for the encapsulation process.

interactions can reduce oxygen diffusion and improve the stability of bioactive compounds during spray drying and subsequent storage.

The collective results demonstrate that encapsulation performance is governed by the dynamic interplay between convective evaporation and diffusive solute migration. The formation of microcapsules is an optimal process, contingent upon the synchronized regulation of three factors: the drying kinetics, the droplet residence time, and the polymer matrix continuity. This integrated understanding provides a predictive engineering framework for the rational design of spray-dried encapsulation systems.

Beyond statistical optimization, the optimized conditions also have practical relevance because the selected core-to-wall ratio, inlet temperature, and feed flow rate were within an operationally feasible range for conventional spray-drying systems. The high encapsulation efficiency and improved polyphenol stability obtained under these conditions support the potential use of the MD + PS formulation in functional food ingredients and bioactive delivery systems. In addition, the use of brewer's spent yeast-derived polysaccharide-rich fraction contributes to by-product valorization and circular bioeconomy development. However, further pilot-scale validation and long-term storage studies in real food matrices are required to confirm industrial applicability.

3.2 Microstructural evolution and barrier properties

SEM micrographs (Fig. 3) show predominantly spherical particles with surface wrinkles and indentations. This morphology is indicative of the spray drying process, wherein rapid crust formation at elevated inlet temperatures is followed by sustained internal moisture evaporation. The resultant volumetric shrinkage generates compressive stresses, leading to surface collapse and wrinkling. The extent of deformation is governed by drying kinetics: higher inlet temperatures or lower solid content accelerate shell formation relative to core dehydration, amplifying structural distortion.[36,37] Consequently, the observed "wrinkled" morphology reflects rapid water diffusion and non-uniform shell–core contraction.

Formulations incorporating yeast-derived polysaccharides exhibited smoother surfaces and fewer fractures than maltodextrin-only systems, indicating enhanced matrix cohesion. The β-glucan backbone is hypothesized to have increased hydrogen-bond density within the wall matrix, while mannoproteins stabilized droplet interfaces prior to drying, promoting homogeneous shell formation. This reinforced microstructure has been demonstrated to reduce microcrack formation and structural discontinuities.

Such a densification process has been shown to enhance the performance of the barrier. A compact hydrogen-bonded network decreases free volume and restricts molecular mobility, thereby lowering effective oxygen diffusivity and solvent ingress. This mechanistic explanation provides a clear rationale for the enhanced oxidative stability observed in polysaccharide-containing formulations.

The FTIR spectra of the spray-dried powder (Fig. 4) confirm the successful encapsulation process. The presence of characteristic polyphenol peaks was observed at 1240 cm^{-1} (O–H stretching of phenols) and 1633 cm^{-1} (aromatic C=C). β-Glucan exhibited a typical band at 1040 cm^{-1} ((C–O–C)/(C–C) vibrations), while the 1560 cm^{-1} peak (amide II) indicated protein presence. The coexistence of these characteristic bands indicates that both polyphenols and yeast-derived polysaccharides were retained within the microcapsule matrix.

3.3 Stability under thermal, photochemical, and oxidative stress

The stability of polyphenol under various forms of stress, including thermal, photochemical, and oxidative stress, was examined. The encapsulation process was found to have a significant impact on the stability of polyphenol under these environmental stressors. From a physicochemical standpoint,

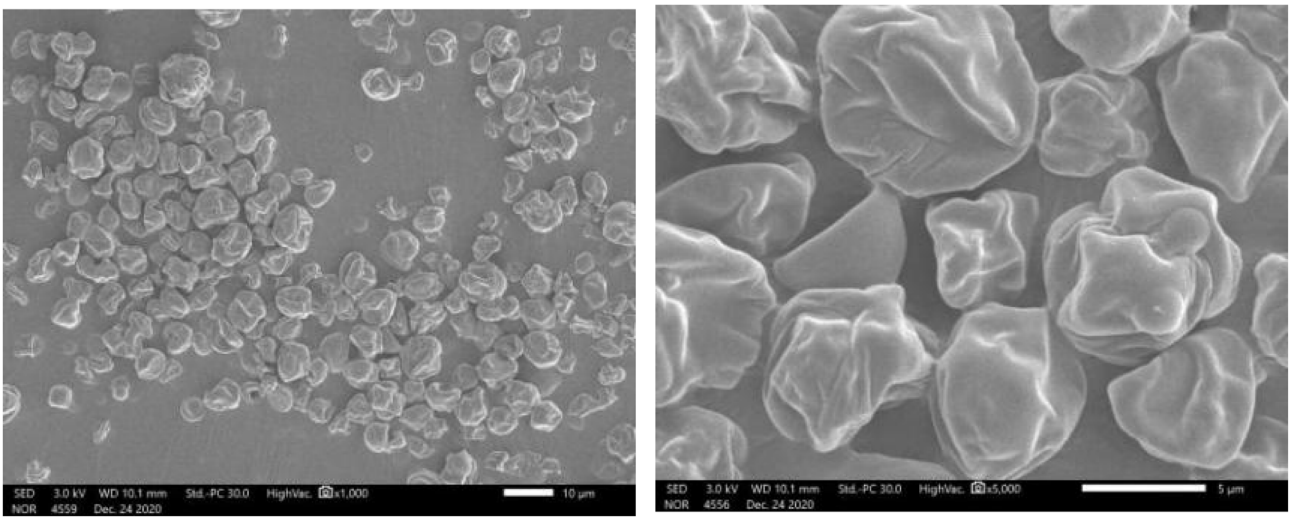

Fig. 3 SEM micrographs of encapsulated polyphenol particles at 30 kV and magnifications of 1000× and 5000×.

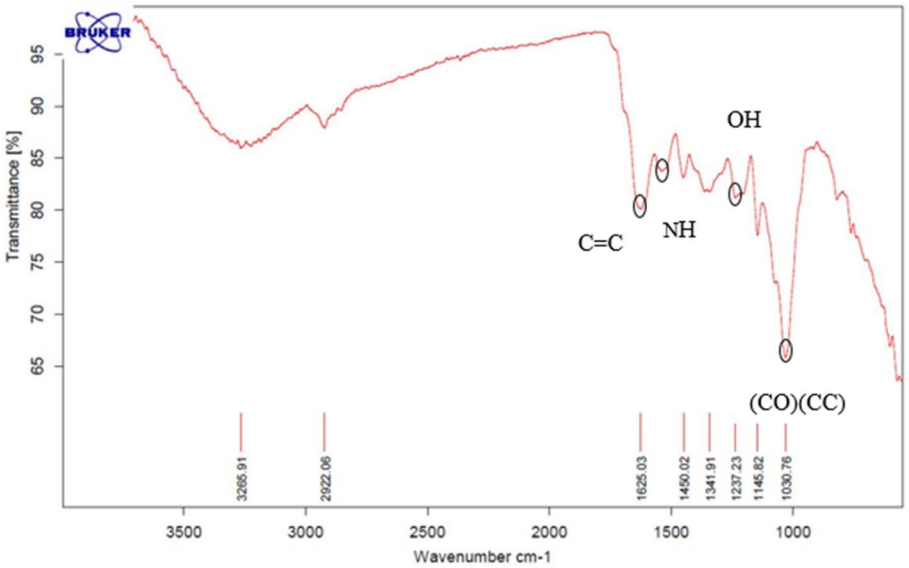

Fig. 4 FTIR spectrum of the spray-dried microencapsulated powder.

degradation follows a coupled reaction-diffusion mechanism in which external stimuli (heat, light, oxygen, *etc.*) accelerate molecular oxidation, structural rearrangement, and radical-mediated chain reactions. The yeast-derived polysaccharide matrix functions as a multifunctional barrier by (i) constraining mass transfer of reactive species, (ii) diminishing molecular mobility through hydrogen-bonding interactions, and (iii) physically entrapping polyphenols within a dense network.

In order to maintain logical coherence, stress factors are discussed in the sequence of intrinsic molecular destabilization (thermal), photo-induced degradation (photochemical), and external oxidative diffusion (oxygen), reflecting increasing environmental complexity.

3.3.1 Effect of temperature. Thermal treatment (70–100 °C; 1–3 h) markedly influenced the stability of TPC and antioxidant activity in both the encapsulated powder and the free extract (Fig. 5). As the temperature and exposure time increased, a progressive decline in TPC and DPPH radical scavenging activity was observed in both systems. This decline was consistent with thermally induced oxidative degradation following Arrhenius-type kinetics. However, the encapsulated samples exhibited a substantially higher retention capacity compared to the non-encapsulated extract, suggesting that the encapsulating matrix plays a crucial role in protecting the extract's properties.

As demonstrated in Fig. 5, TPC decreased gradually with increasing temperature and prolonged heating time. At 70 °C, the microencapsulated sample retained over 81.90% of its initial TPC after a duration of 3 h. In contrast, the free extract demonstrated a retention of only 20.20%, thereby substantiating the substantial thermal vulnerability of unprotected polyphenols. At 80 °C, encapsulated TPC remained relatively stable after 1 h (89.88%) and 2 h (84.87%), before declining to 71.04% at 3 h. Conversely, the extract exhibited a sharp reduction in TPC from 57.87% (1 h) to 19.96% (3 h). The discrepancy between the two systems became more evident at 90 °C and 100 °C. At 90 °C, the encapsulated TPC decreased from 80.74% (1 h) to 48.35% (3 h), while in the extract it dropped dramatically to 11.42% after 3 h. At 100 °C, the degradation was most severe, with encapsulated samples retaining only 21.38% TPC after 3 h compared with 9.93% TPC for the extract. These findings confirm that polyphenols are highly thermolabile compounds and that degradation accelerates in response to elevated thermal intensity and duration.

The pattern of antioxidant activity reflected the reduction in TPC, suggesting that phenolic compounds were the primary contributors to radical scavenging capacity (Fig. 5). At 70 °C, the encapsulated powder maintained 72.88% DPPH scavenging activity after 3 h, whereas the extract retained only 20.30% of its activity. Even at 80 °C, the encapsulated system preserved 50.48% activity after 3 h, in contrast to the 18.31% activity observed for the extract. At 90 °C, antioxidant activity of the microcapsules remained relatively stable up to 2 h (62.54%) but declined sharply to 41.60% at 3 h. At 100 °C, DPPH activity of the encapsulated sample fell below 50% after 2 h (36.67%) and further to 20.15% after 3 h. The free extract exhibited more pronounced degradation, particularly at 90–100 °C, where the activity decreased to approximately 10% after 3 h. The parallel reduction of TPC and DPPH activity indicates that thermal degradation likely involves oxidative cleavage, structural rearrangement, or polymerization of phenolic hydroxyl groups, resulting in diminished radical-scavenging efficiency.

Mechanistically, the enhanced thermal stability of encapsulated polyphenols can be attributed to the physicochemical properties of the polysaccharide matrix. The rigid network structure likely reduces molecular mobility, limits oxygen diffusion, and restricts radical propagation pathways. Furthermore, encapsulation may increase the apparent activation energy required for degradation by confining polyphenols within a protective microenvironment, thereby reducing

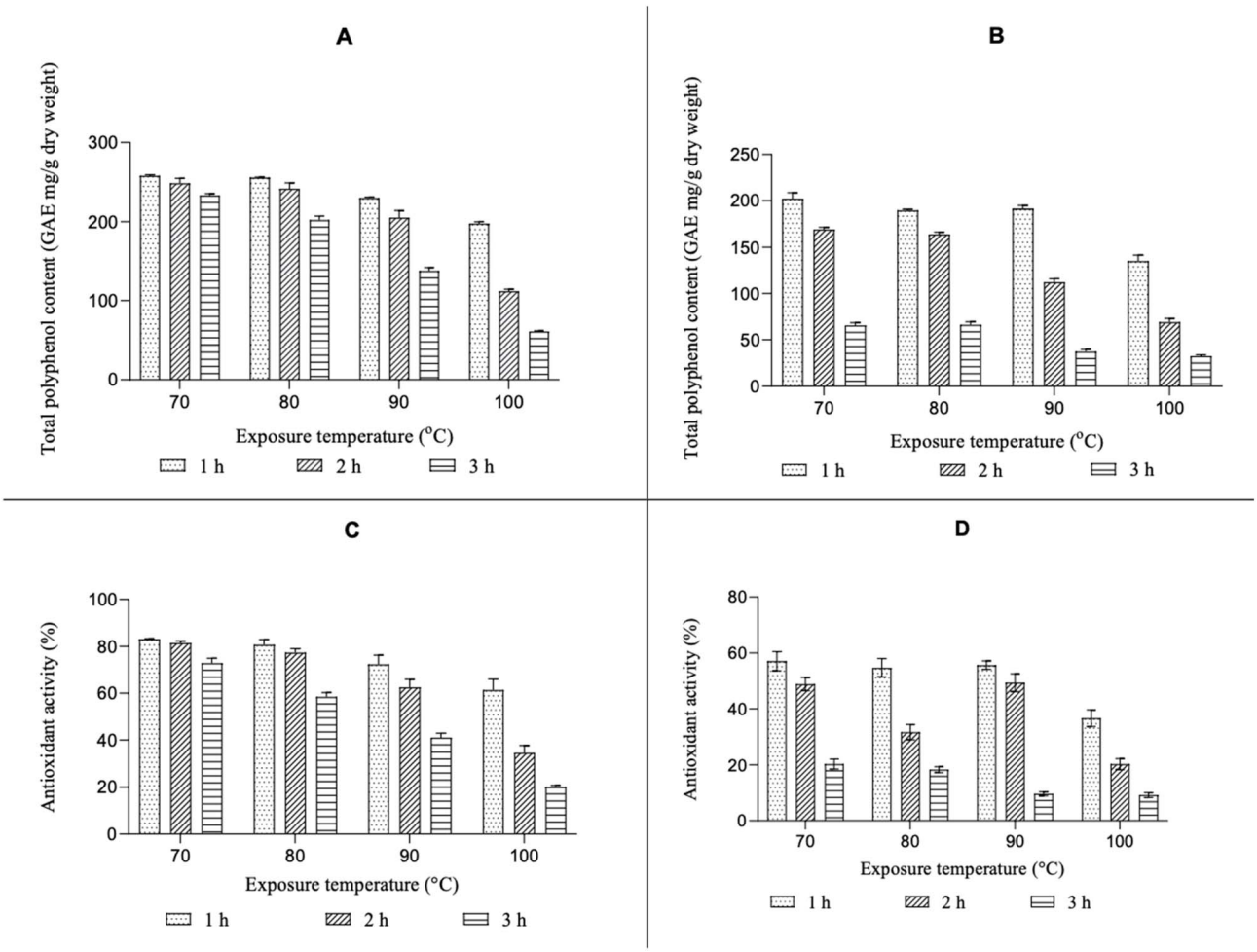

Fig. 5 Effect of temperature on total phenolic content and antioxidant activity of the encapsulated powder and free extract ((A and C) encapsulated powder; (B and D) free extract).

exposure to heat and oxidative stress. The reduced surface migration and volatilization of low-molecular-weight phenolics may also contribute to improved retention. The protective effect was particularly evident within the moderate temperature range of 70–90 °C for up to 2 h. Beyond this time, structural relaxation and matrix softening at higher temperatures (100 °C) likely compromised barrier integrity.

These findings are consistent with the results of previous studies that reported temperature-dependent decreases in phenolic antioxidant activity. Réblová[38] demonstrated that increasing the temperature from 90 to 150 °C significantly reduced the phenolic antioxidant capacity due to thermal decomposition and oxidation. Similarly, Wang *et al.*[39] reported improved thermal stability of microencapsulated tea polyphenols compared with free polyphenols, particularly under moderate heating conditions. The present results align with those observations, thereby further confirming that microencapsulation is an effective strategy for enhancing the thermal resilience of phenolic compounds.

3.3.2 Effect of light. Exposure to light is a critical environmental factor influencing the stability of phenolic compounds due to photo-oxidative reactions initiated by photon absorption. When phenolic chromophores absorb light energy, excited states are generated, facilitating the formation of reactive oxygen species (ROS), which subsequently promote oxidative degradation. In the present study, the spray-dried microencapsulated powder and free extract were exposed to illumination intensities of 10 000, 22 000, and 34 000 Lux for up to 9 days, and changes in TPC and antioxidant activity (DPPH assay) were monitored.

As illustrated in Fig. 6, both systems exhibited progressive reductions in TPC and antioxidant capacity over time, with degradation strongly dependent on light intensity. However, the extent of degradation was consistently lower in the microencapsulated samples compared with the free extract. After 9 days of storage under 10 000 Lux, TPC in the microencapsulated powder decreased by approximately 16.60%, whereas the extract showed a reduction of 41.36%. At 22 000 Lux, TPC losses reached about 18.83% in the encapsulated sample and 52.19% in the extract. The most pronounced degradation occurred at 34 000 Lux, where TPC declined by 29.59% in the microcapsules compared with 55.65% in the extract. These results clearly

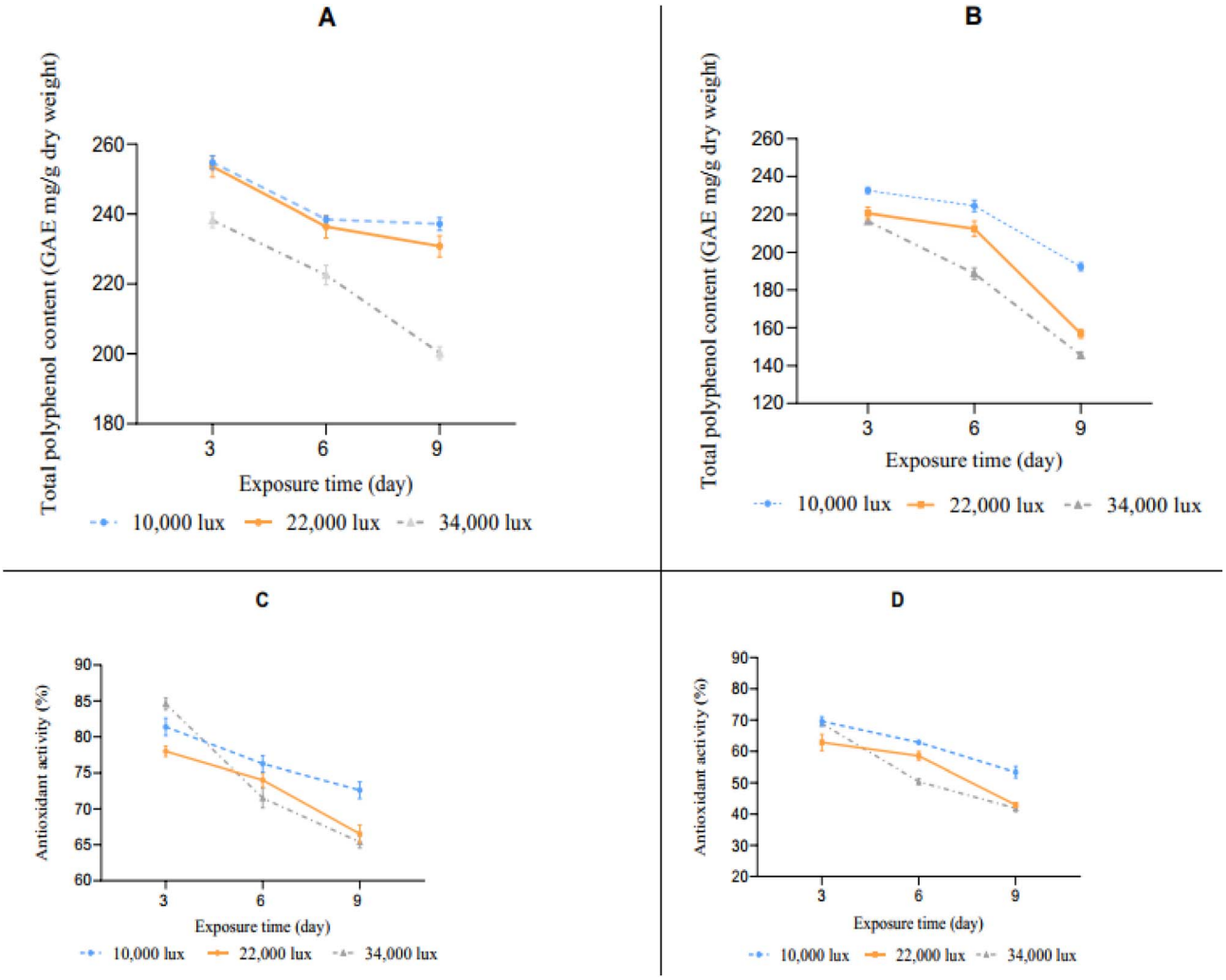

Fig. 6 Effect of light exposure on total polyphenol content and antioxidant activity of microencapsulated powder and free extract ((A and C) encapsulated powder; (B and D) free extract).

demonstrate that increasing light intensity accelerates phenolic degradation and that encapsulation significantly mitigates this effect.

A similar trend was observed for antioxidant activity. After 9 days at 10 000 Lux, DPPH scavenging activity decreased by approximately 20.29% in the microencapsulated sample and 43.21% in the extract. At 22 000 Lux, reductions reached 26.36% and 53.68%, respectively, while at 34 000 Lux the decreases were 27.50% for the microcapsules and 54.72% for the extract. The parallel decline of TPC and antioxidant activity indicates that phenolic compounds are the principal contributors to radical-scavenging capacity. The strong correlation between these parameters suggests that photo-induced structural modifications, such as hydroxyl group oxidation, quinone formation, or phenolic ring cleavage, directly impair antioxidant functionality.

Notably, under moderate illumination (10 000 Lux), the protective effect of encapsulation was particularly evident. After 9 days, the TPC and DPPH values in the microencapsulated powder remained above 80%, whereas the extract retained only slightly above 60%. At higher intensities (22 000–34,000 Lux), the divergence between the two systems became more pronounced, with encapsulated samples maintaining TPC above 70%, while the extract fell below 60%. The minimal changes observed in the control samples confirm that degradation in experimental groups was primarily attributable to light exposure rather than intrinsic instability.

The enhanced photostability of the encapsulated system can be attributed to several physicochemical mechanisms. The PS matrix likely acts as a physical light-scattering and diffusion barrier, reducing photon penetration and limiting direct excitation of phenolic chromophores. Additionally, hydrogen bonding and hydrophobic interactions between polyphenols and the matrix may restrict molecular mobility and stabilize phenolic hydroxyl groups, thereby decreasing susceptibility to photo-oxidation. Reduced oxygen diffusion within the microcapsule structure may further suppress ROS-mediated degradation pathways. Collectively, these mechanisms increase the effective resistance of polyphenols to photo-induced oxidative reactions.

These findings are consistent with previous reports highlighting the vulnerability of phenolic compounds to light exposure.[40] It has been emphasized that light-induced ROS generation is a major pathway for phenolic degradation. Similarly, Shi *et al.*[2] reported that microencapsulation improved the photostability of resveratrol under fluorescent light, with retention levels remaining substantially higher than in the free form. The present results corroborate these observations and confirm that microencapsulation is an effective strategy for enhancing the photochemical stability of polyphenols.

3.3.3 Effect of oxygen. The oxidative stability of spray-dried microencapsulated powder and free extract was evaluated under both ambient and vacuum packaging conditions over a storage period of 3–9 days. The TPC and antioxidant activity were monitored, and the results are presented in Fig. 7. Overall, both TPC and antioxidant activity exhibited a decreasing trend over time across all treatments, indicating progressive oxidative degradation during storage. However, the rate and magnitude of degradation differed markedly depending on the encapsulation and packaging conditions.

Under ambient storage conditions, degradation was found to be significantly more pronounced in the free extract compared to the microencapsulated powder. After 6 and 9 days, there was an approximately 17.12% and 21.39% decrease in TPC in the encapsulated samples, respectively, whereas the free extract exhibited reductions of about 29.53% and 42.93% over the same intervals. A comparable trend was noted in antioxidant activity: the encapsulated powder declined by 15.11% and 17.88% after 6 and 9 days, respectively, while the free extract decreased more sharply by 21.77% and 44.11%, respectively. Notably, the decline during the first three days was relatively modest for all samples, followed by a more accelerated reduction between days 6 and 9. This dynamic behavior suggests that the diffusion of oxygen into the matrix and the subsequent radical-mediated

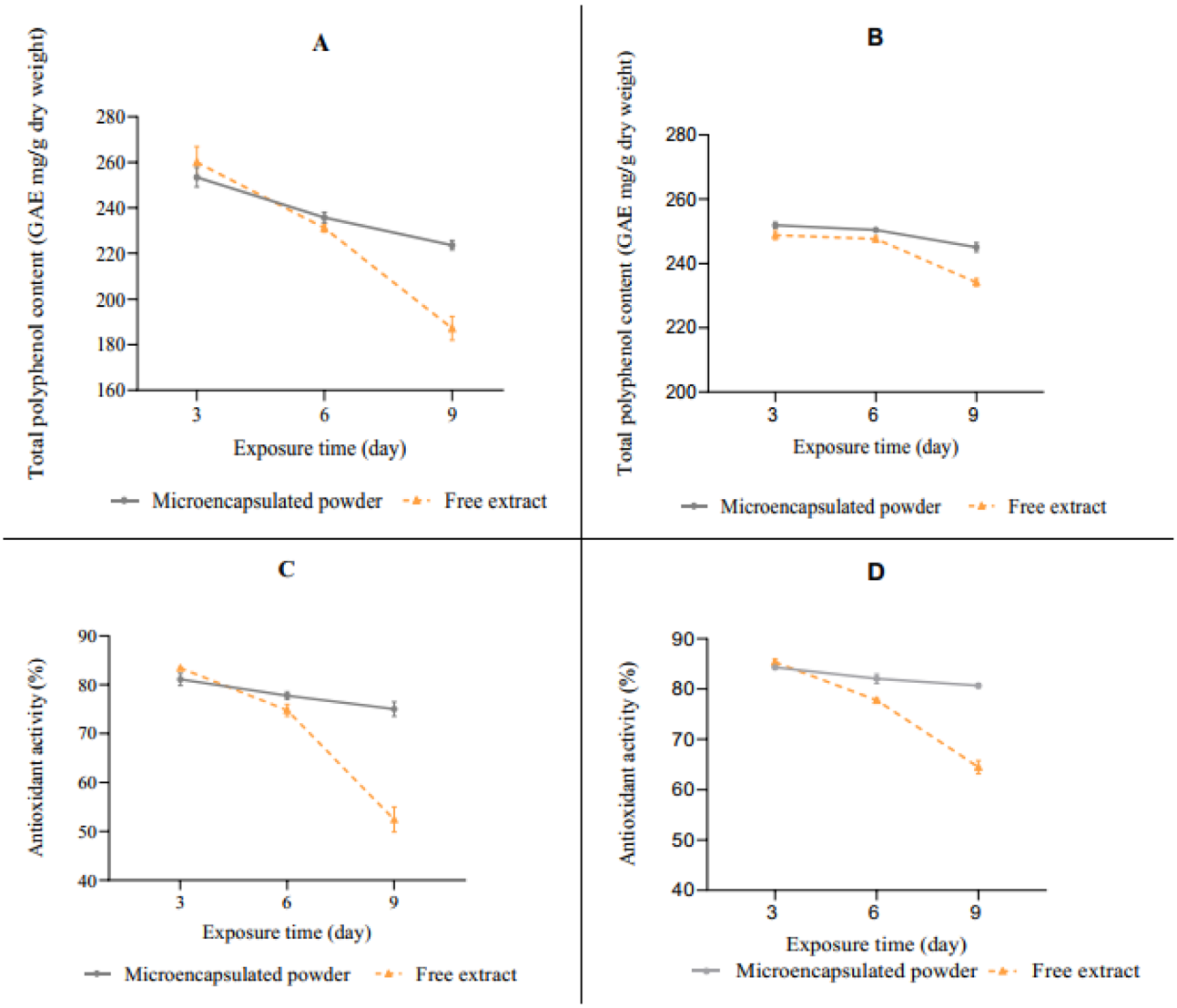

Fig. 7 Effect of oxygen on total polyphenol content and antioxidant activity of free extract and microencapsulated powder during storage. (A and C) Encapsulated powder under ambient conditions; (B and D) encapsulated powder under vacuum conditions.

oxidation reactions become increasingly significant as storage progresses.

Under vacuum conditions, the extent of degradation was markedly reduced. After 9 days, TPC in the microencapsulated powder decreased by only 13.88%, compared with 28.59% in the free extract. Antioxidant activity showed a similar trend: the encapsulated sample declined by approximately 12.20%, whereas the free extract exhibited a substantially greater reduction (32.04%). These findings confirm that oxygen availability is the dominant factor governing polyphenol degradation. Limiting oxygen exposure effectively suppresses oxidative reactions, thereby preserving both phenolic content and bioactivity.

Mechanistically, the degradation of polyphenols can be attributed to their intrinsic redox properties. As potent antioxidants, polyphenols readily react with molecular oxygen and reactive oxygen species, leading to structural modification and the formation of oxidized derivatives. In non-encapsulated extracts, direct exposure to oxygen facilitates rapid oxidation, resulting in a measurable decrease in TPC and antioxidant capacity. This phenomenon has been widely reported in the literature, including the work of Munin and Edwards-Lévy,[40] who described the susceptibility of bioactive compounds to oxidative degradation in unprotected systems.

In contrast, the spray-dried microcapsules exhibited significantly improved stability. The enhanced protection can be attributed to the structural characteristics of the encapsulating material. PS extracted from yeast possesses a unique three-dimensional network capable of forming a protective matrix around entrapped polyphenols. This matrix increases diffusional tortuosity, reduces oxygen permeability, and decreases the free volume available for molecular transport. Consequently, the effective oxygen diffusivity within the system is lowered, suppressing radical chain initiation and propagation reactions. The hydrogen-bonded β-glucan network likely contributes to this barrier effect, thereby maintaining the structural integrity and biological activity of the encapsulated polyphenols.

It should be noted that TPC and DPPH results were influenced by the recovery of phenolics from different sample matrices. Because the free extract and encapsulated powders differed in physical structure, matrix-specific extraction solvents were used to ensure phenolic recovery prior to analysis. Therefore, TPC values are interpreted as recoverable total phenolic content, while DPPH values represent apparent radical-scavenging activity under the specified extraction and dilution conditions. Accordingly, the discussion emphasizes relative retention and stability trends rather than direct solvent-independent comparison of absolute values. Future studies should include matrix-matched recovery validation and antioxidant activity normalized to phenolic concentration.

Taken together, the results clearly demonstrate that microencapsulation significantly mitigates oxygen-induced degradation of polyphenols under both ambient and vacuum storage conditions. The parallel decline observed between TPC and antioxidant activity further supports the strong correlation between the phenolic concentration and radical scavenging capacity. Therefore, microencapsulation represents an effective strategy for preserving the functional properties of polyphenols during storage by minimizing oxidative loss.

3.4 Release behavior

3.4.1 Release of polyphenols in simulated food media. Polyphenols are chemically labile bioactive compounds that are highly susceptible to oxidative degradation, solvent effects, and pH-induced structural transformation during food processing and storage. Although their redox properties confer antioxidant functionality, these same properties render them vulnerable to rapid degradation in unprotected systems. It has been reported that only approximately 1–2% of orally ingested polyphenols ultimately reach target tissues in their active form.[41] Therefore, encapsulation has been increasingly applied as a technological strategy not only improve polyphenol stability but also to regulate their release under food and gastrointestinal conditions.

The surface morphology of spray-dried microcapsules prepared with MD, MD + SPI, and MD + PS is presented in Fig. 8. The SEM micrographs revealed formulation-dependent differences in particle surface characteristics before release testing. The MD particles exhibited relatively smooth and compact surfaces, whereas the MD + SPI particles displayed greater surface irregularity and visible microstructural discontinuities. These features may be associated with differences in wall-

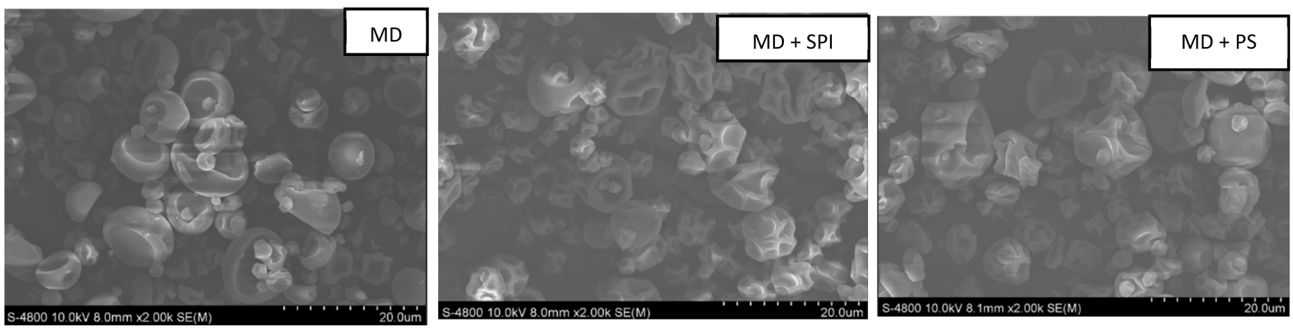

Fig. 8 SEM micrographs of microencapsulated polyphenol particles at 10 kV and 2000× magnification. MD: maltodextrin; MD + SPI: maltodextrin + soy protein isolate; MD + PS: maltodextrin + polysaccharide.

material composition and particle formation during spray drying. The MD + PS particles appeared to show fewer visible surface fractures and a comparatively more continuous morphology. However, these SEM observations should only be interpreted as qualitative evidence of pre-digestion particle morphology, rather than as a direct proof of matrix robustness or structural integrity after digestion. Therefore, the release behavior was interpreted primarily based on wall-material solubility, hydration behavior, matrix swelling, enzymatic susceptibility, diffusional tortuosity, and possible molecular interactions between polyphenols and the carrier matrix. A limitation of the present study is that SEM analysis was performed only on the spray-dried powders before digestion; therefore, post-digestion structural changes were inferred from release behavior rather than directly visualized. Future studies should include post-digestion SEM or complementary structural analyses to confirm matrix erosion, swelling, and integrity during gastrointestinal release.

A limitation of the present study is that SEM analysis was performed only on the spray-dried powders before digestion. Therefore, post-digestion structural changes were inferred from release behavior rather than directly visualized. Future studies should include post-digestion SEM or complementary structural analyses to confirm matrix erosion, swelling, and integrity during gastrointestinal release.

The release profiles in simulated food media are illustrated in Fig. 9A–D. In 10% ethanol (Fig. 9A), significant differences ($p < 0.05$) were observed among formulations and the free extract. The free extract exhibited the lowest apparent recoverable polyphenol level at the initial time point, followed by a further decline over time. Because the free extract was not incorporated into a wall matrix, this value should be interpreted as the

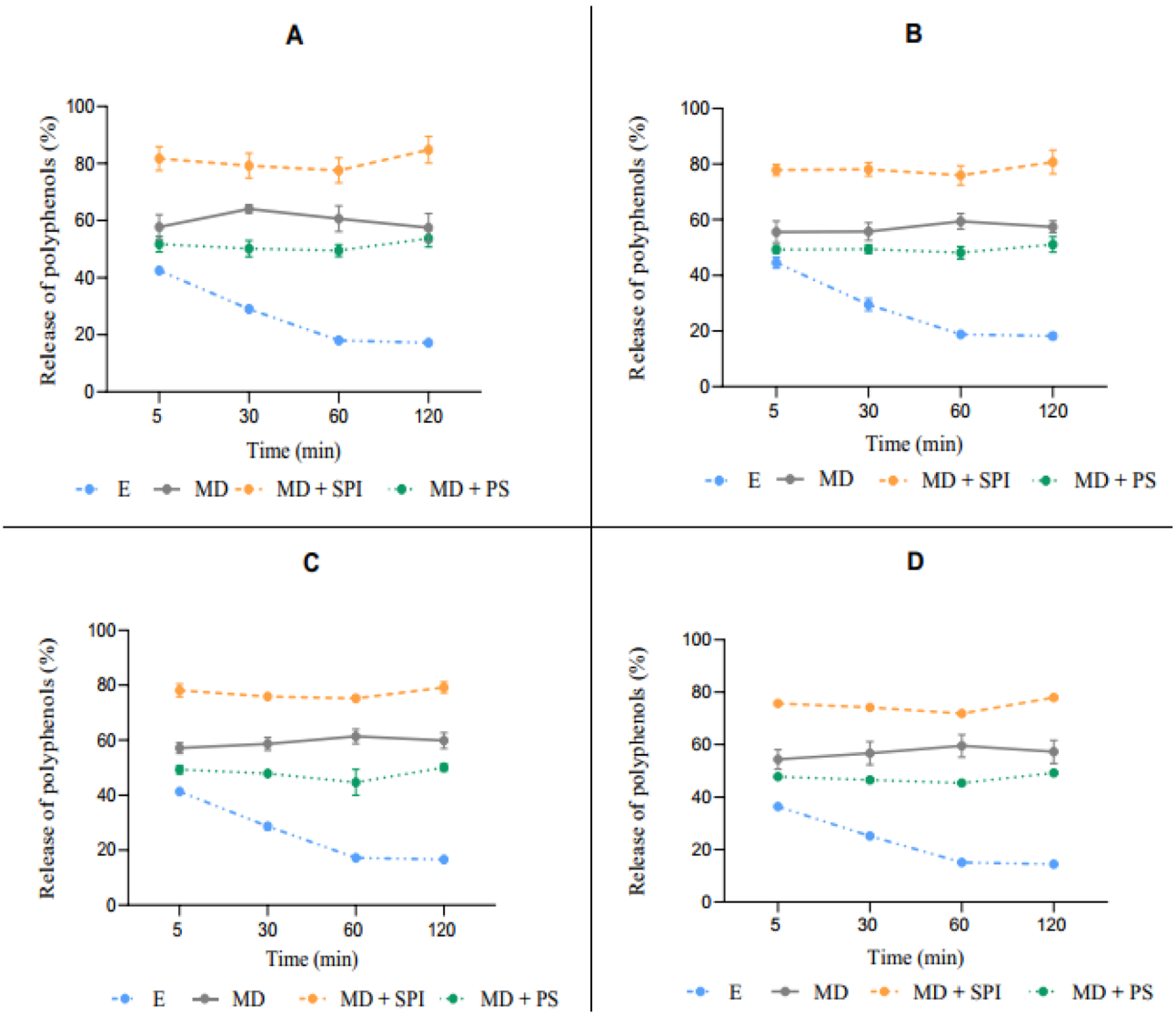

Fig. 9 Apparent release or recoverable polyphenols in simulated food systems from the free extract and different microencapsulation formulations. E: free extract; MD: maltodextrin; MD + SPI: maltodextrin combined with soy protein isolate; MD + PS: maltodextrin combined with the yeast-derived polysaccharide-rich fraction. (A–C) ethanol media at 10%, 20%, and 50%; (D) 3% acetic acid medium. Values are expressed as mean ± standard deviation ($n = 3$).

recoverable phenolic fraction under the tested conditions rather than as release from a microencapsulated system. The low recovery and subsequent decrease suggest that, in the absence of a protective matrix, polyphenols were more susceptible to degradation, oxidation, structural transformation, or interactions with components of the surrounding medium.

By contrast, the encapsulated systems retained higher levels of measurable polyphenols, although their release profiles differed markedly depending on wall material composition. The MD + SPI formulation achieved the highest apparent release level, exceeding 80% under this condition. This behavior may be associated with rapid hydration of the maltodextrin-rich phase and partial swelling or relaxation of the carbohydrate–protein matrix, which facilitated solvent penetration and polyphenol diffusion. The MD-only system showed an intermediate apparent release level of approximately 55–60%, suggesting that release was governed mainly by hydration, matrix dissolution, and diffusion. Meanwhile, the MD + PS system exhibited a lower and more gradual apparent release level of approximately 50–55%, indicating that the yeast-derived polysaccharide-rich matrix may have restricted solvent ingress and delayed polyphenol migration. This interpretation is consistent with diffusion-based mass-transfer behavior, in which solvent penetration, matrix relaxation, and bioactive diffusion collectively govern release from polymeric matrices.[42]

A similar ranking order of apparent release (MD + SPI > MD > MD + PS) was observed in 20% ethanol (Fig. 9B) and 50% ethanol (Fig. 9C), although the overall release levels decreased moderately as the ethanol concentration increased. This decrease may be related to reduced solvent polarity, lower polyphenol solubility, and decreased effective diffusion coefficients, thereby limiting mass transfer from the particles into the surrounding medium. Nevertheless, the relative consistency ranking among the encapsulated systems across ethanol concentrations suggests that matrix composition and structural properties had a stronger influence on release kinetics than solvent polarity alone within the tested range. The consistently lower recovery of the free extract further confirms the importance of encapsulation for maintaining measurable polyphenols during exposure to food-simulating media.

In an acidic medium containing 3% acetic acid (Fig. 9D), the free extract again showed rapid initial availability followed by a substantial reduction in recoverable polyphenols. This result suggests that acid-induced structural transformation and chemical instability contributed to polyphenol loss in the unprotected system. Encapsulation significantly improved stability under these conditions, but the extent of release remained formulation dependent. Although hydrophilic carriers may swell and release bioactives more rapidly under acidic environments,[43] the MD + PS formulation displayed comparatively restrained release. This behavior may be ascribed to the greater structural resilience of the β-glucan and mannan-containing yeast cell wall matrix, which may limit acid-induced matrix erosion and diffusion-driven transport.

The formulation-dependent release behavior can be further explained by the differences in polymer solubility, hydration rate, matrix cohesion, and molecular interactions. The rapid and extensive release observed in the MD + SPI system was likely associated with the high aqueous solubility of maltodextrin and the rapid hydration of the carrier phase. Maltodextrin-rich matrices can absorb water readily and undergo fast dissolution or structural weakening upon contact with aqueous media, thereby promoting solvent ingress and outward diffusion of polyphenols.[44] In addition, spray-dried MD-based particles may contain porous or less cohesive regions, which further facilitate mass transfer. Although SPI can contribute film-forming properties, the protein phase may undergo conformational changes during drying and structural relaxation in aqueous environments, reducing matrix integrity and accelerating release.[45] Furthermore, interactions between maltodextrin and polyphenols are mainly governed by relatively weak non-covalent interactions, particularly hydrogen bonding, which may be insufficient to maintain strong retention of the bioactive compounds.[8] These factors collectively explain the pronounced initial release observed in the MD + SPI formulation.

In contrast, the slower release from the MD + PS system can be attributed to the formation of a more cohesive β-glucan/mannoprotein-rich network.[9] This polysaccharide matrix may increase diffusional tortuosity, restrict solvent penetration, reduce molecular mobility, and retain polyphenols through hydrogen bonding and other weak intermolecular interactions.[7] Moreover, controlled swelling of the polysaccharide-rich matrix may support a diffusion–relaxation-controlled release mechanism rather than an immediate dissolution-driven process.[46] Therefore, the MD + PS formulation provided a more gradual and controlled release profile, indicating that the yeast-derived polysaccharide-rich fraction can act not only as a protective wall material but also as a release-modulating biopolymer matrix.

3.4.2 Release behavior under simulated gastrointestinal conditions. The gastrointestinal tract presents a complex environment characterized by drastic pH variation, ionic strength variation, and enzymatic activity, all of which can compromise polyphenol stability and bioavailability. It has been reported that only a limited proportion of ingested polyphenols (5–10%) is absorbed in the small intestine.[47] Consequently, controlled-release systems are important for improving the protection, retention, and intestinal availability of polyphenols.

The release profiles in simulated gastric fluid (SGF, pH 1.2) and simulated intestinal fluid (SIF, pH 6.8) are presented in Fig. 10, respectively. In SGF (Fig. 10), the free extract exhibited an immediate burst-type release (>90% at 5 min), followed by a rapid decline in recoverable polyphenols. This pattern indicates the poor acid stability of the non-encapsulated extract and suggests that degradation or structural transformation occurred rapidly after exposure to gastric conditions. In contrast, the encapsulated formulations displayed biphasic release behavior, consisting of an initial release phase, probably associated with surface-associated or weakly bound polyphenols, followed by a slower release phase governed by diffusion through the hydrated matrix.

The MD-only system showed substantial early release followed by a pronounced decrease in recoverable polyphenols, indicating limited protection against acid-mediated degradation. This behavior is consistent with the rapid hydration and

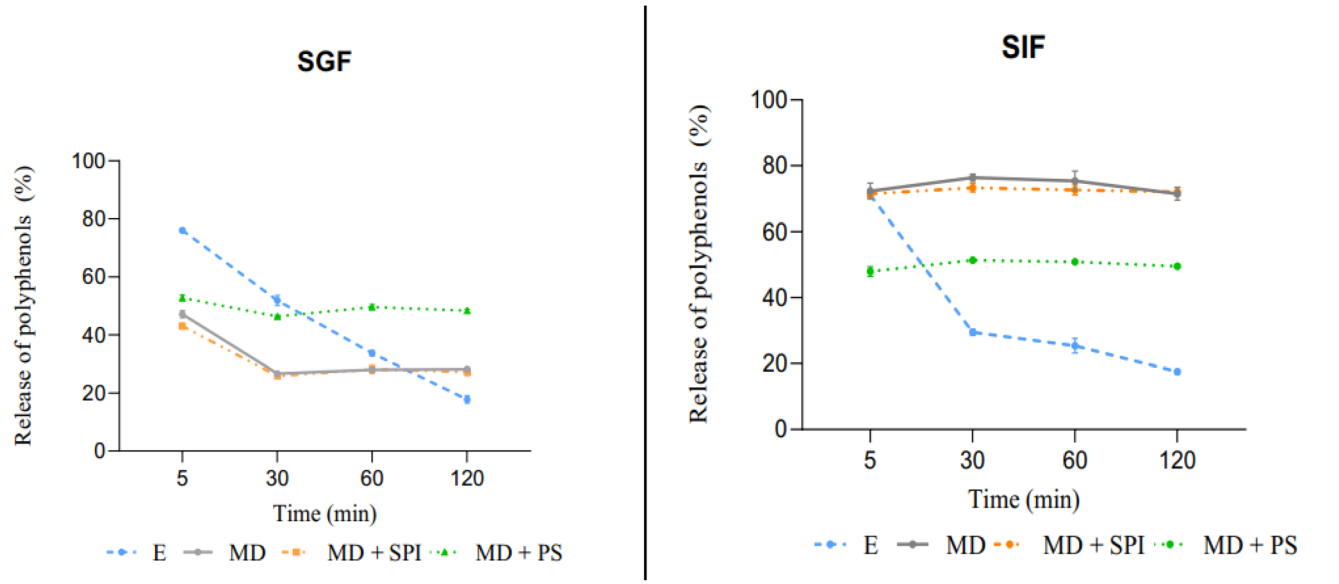

Fig. 10 Percentage release of polyphenols in simulated gastrointestinal media from the free extract and different microencapsulation formulations. E: free extract; MD: maltodextrin; MD + SPI: maltodextrin combined with soy protein isolate; MD + PS: maltodextrin combined with yeast-derived polysaccharide-rich fraction; SGF: simulated gastric fluid; SIF: simulated intestinal fluid. Values are expressed as mean ± standard deviation ($n = 3$).

partial structural weakening of maltodextrin matrices in aqueous acidic environments, which can promote premature diffusion of entrapped compounds.[48] Although differences in formulation and experimental design may influence the release magnitude, the overall trend suggests that single-component MD matrices provide limited gastric resistance. The MD + SPI formulation exhibited a more moderate release profile than MD alone; however, the protein-containing matrix may be susceptible to pepsin-mediated hydrolysis, which can weaken the matrix and increase the diffusion pathways during gastric exposure.[49] In contrast, the MD + PS system maintained a more restrained and sustained release profile throughout the gastric simulation. These findings suggest that the yeast-derived polysaccharide matrix is more resistant to rapid acid-induced disruption under the tested conditions.

Under simulated intestinal conditions (Fig. 10), the free extract exhibited a rapid but unstable release pattern, followed by a marked decline in recoverable polyphenols over time. This release may be attributed to the poor stability of non-encapsulated polyphenols under intestinal pH and enzymatic conditions, as well as possible oxidative degradation or interaction with components of the simulated intestinal fluid. In contrast, the encapsulated systems improved polyphenol retention and modulated release kinetics to different extents. The MD and MD + SPI formulations reached relatively high apparent release levels of approximately 70–75%, indicating faster matrix hydration and diffusion of polyphenols into the surrounding medium. In the MD + SPI system, this release may have been further accelerated by the susceptibility of the protein phase to enzymatic hydrolysis by pancreatin, which can promote matrix erosion and open additional diffusion pathways.

The MD + PS system exhibited a more controlled and sustained release profile, with an apparent release level of approximately 50%. This behavior suggests that the β-glucan/mannoprotein-rich matrix was less susceptible to rapid enzymatic disruption under the tested intestinal conditions. The polysaccharide network may hydrate and swell gradually while maintaining sufficient structural integrity to delay solvent penetration and polyphenol diffusion. Such matrix-dependent behavior is consistent with previous reports, showing that polysaccharide-based encapsulation systems can enhance bioactive stability and regulate release kinetics.[50,51] Therefore, polyphenol release from the MD + PS system was likely governed by coupled diffusion and polymer relaxation, rather than by rapid matrix dissolution or enzymatic erosion alone.

Overall, the release behavior observed in the simulated food and gastrointestinal environments (Fig. 9 and 10) was governed by a multifactorial interplay among solvent polarity, matrix hydration, diffusional tortuosity, polymer solubility, and enzymatic susceptibility. The MD + SPI formulation favored relatively rapid bioactive availability because of hydration-driven diffusion and possible protein-phase degradation under enzymatic conditions. Conversely, the MD + PS system provided a slower and more controlled release pattern, particularly under gastrointestinal conditions, likely due to the cohesive β-glucan/mannoprotein-rich network. These findings confirm that microencapsulation not only enhances polyphenol stability but also enables formulation-specific modulation of release behavior for potential functional food and nutraceutical applications.

Nevertheless, the interpretation of these results should be considered within the limitations of the present study. SEM observations were obtained before digestion; therefore, post-

digestion structural changes were inferred from release behavior rather than direct visualization. In addition, the yeast-derived polysaccharide fraction contained residual protein, which may have contributed to matrix formation and polyphenol binding. Future studies should include post-digestion morphology, molecular-weight distribution, rheological characterization, swelling measurements, and kinetic modelling to more precisely distinguish the relative contributions of diffusion, polymer relaxation, and matrix erosion to polyphenol release.

4 Conclusions and recommendations

This study elucidated the interrelationship between spray-drying parameters, matrix microstructure, and transport-governed release behavior of polyphenols encapsulated in maltodextrin and yeast-derived polysaccharide systems. The process optimization resulted in the formation of structurally coherent microcapsules, exhibiting high encapsulation efficiency and reduced surface migration of bioactive compounds. Spectroscopic and morphological analyses confirmed the successful entrapment and particle formation, while environmental stability tests highlighted the sensitivity of polyphenols to oxygen, light, and temperature. Notably, incorporation of polysaccharide enhanced matrix cohesion, decreased effective diffusivity, and shifted the release mechanism from predominantly Fickian diffusion to anomalous diffusion, indicating coupled diffusion–polymer relaxation behavior.

Under simulated gastrointestinal conditions, encapsulated formulations demonstrated superior protection and more controlled release compared with the free extract, which exhibited rapid apparent availability followed by a decline in recoverable phenolics, probably due to degradation or instability in the gastrointestinal media. These findings establish a clear process–structure–function relationship and support the valorization of yeast-derived polysaccharide-rich fraction as structurally robust and sustainable encapsulating agents. Future research should include post-digestion structural characterization, *in vivo* bioavailability validation, long-term storage assessment in real food systems, and scale-up evaluation to facilitate industrial translation.

Author contributions

Hien Thi Do: writing – original draft preparation, investigation, methodology, data curation, formal analysis, validation; Tuyen Chan Kha: conceptualization, methodology, writing – review & editing, supervision. All authors have read and agreed to the published version of the manuscript.

Conflicts of interest

The authors state that there are no conflicts to declare.

Data availability

The data supporting the findings of this study are included within the article.

Acknowledgements

The authors gratefully acknowledge the valuable assistance of Mr Nguyen Vinh Khang, Ms. Vo Thanh Duyen, Ms Nguyen Thi Minh Thu, and Ms Vo Thi Kim Ngan in sample analysis. The authors also sincerely thank Ho Chi Minh City University of Industry and Trade for providing the facilities and equipment necessary to conduct this research.

References

1 Z. Piñeiro, M. Palma and C. G. Barroso, *J. Chromatogr. A*, 2006, **1110**, 61–65.
2 G. Shi, L. Rao, H. Yu, H. Xiang, H. Yang and R. Ji, *Int. J. Pharm.*, 2008, **349**, 83–93.
3 A. T. Vu and T. C. Kha, in *Synthesis of Nanomaterials*, ed. F. López-Saucedo, Bentham Science Publisher, Singapore, 2023, vol. 3, pp. 222–258.
4 A. T. Vu, T. C. Kha and H. T. Phan, *Foods*, 2024, **13**, 100.
5 G. Kogan and A. Kocher, *Livest. Sci.*, 2007, **109**, 161–165.
6 B. Podpora, F. Świderski, A. Sadowska, R. Rakowska and G. Wasiak-Zys, *Czech J. Food Sci.*, 2016, **34**, 554–563.
7 C. Le Bourvellec and C. M. Renard, *Crit. Rev. Food Sci. Nutr.*, 2012, **52**, 213–248.
8 L. Jakobek, *Food Chem.*, 2015, **175**, 556–567.
9 T. Bohn, *Nutr. Rev.*, 2014, **72**, 429–452.
10 S. Rehman, A. H. Gora, Q. u. Ain, S. Muhammed, B. Xavier K, N. K. Sanil, K. Sharma S R and K. Chakraborty, *Front. Microbiol.*, 2026, **17**, 1719665.
11 E. Díaz-Montes, *Polymers*, 2023, **15**, 2659.
12 Y. Chen, Y. Liu, W. Han, Y. Huang, Y. Song, D. Li and M. Tan, *Trends Food Sci. Technol.*, 2026, **172**, 105739.
13 D. E. Laib, I. Laib, H. Bendif, S. A. Alsalamah, T. H. Taha, F. Boufahja, W. Elfalleh and S. Garzoli, *Food Sci. Biotechnol.*, 2026, **35**, 1467–1482.
14 A. Czerniak, P. Kubiak, W. Białas and T. Jankowski, *J. Food Eng.*, 2015, **167**, 2–11.
15 A. Sultana, Y. Tanaka, Y. Fushimi and H. Yoshii, *Food Res. Int.*, 2018, **106**, 809–816.
16 Y. T. Dang, H. Tran and T. C. Kha, *Foods*, 2024, **13**, 1463.
17 N. Ramesh and A. K. A. Mandal, *Drug Dev. Ind. Pharm.*, 2019, **45**, 1506–1514.
18 M. Saifullah, R. McCullum, T. O. Akanbi and Q. Van Vuong, *Food Hydrocolloids Health*, 2023, **4**, 100157.
19 T. H. Do, T. C. Kha and P. P. T. Huynh, *HCMCOU J. Sci. – Eng. Technol.*, 2022, **12**, 79–89.
20 M. Friedman, C. E. Levin, S.-H. Choi, E. Kozukue and N. Kozukue, *J. Food Sci.*, 2006, **71**, C328–C337.
21 M.-J. Lu and C. Chen, *Food Res. Int.*, 2008, **41**, 130–137.
22 E. Talón, K. T. Trifkovic, M. Vargas, A. Chiralt and C. González-Martínez, *Carbohydr. Polym.*, 2017, **175**, 122–130.
23 D. Dag, M. Kilercioglu and M. H. Oztop, *LWT–Food Sci. Technol.*, 2017, **83**, 86–94.
24 E. A. Ainsworth and K. M. Gillespie, *Nat. Protoc.*, 2007, **2**, 875–877.

25 P. Robert, T. Gorena, N. Romero, E. Sepulveda, J. Chavez and C. Saenz, *Int. J. Food Sci. Technol.*, 2010, **45**, 1386–1394.
26 G. A. Agbor, J. A. Vinson and P. E. Donnelly, *Int. J. Food Sci. Nutr. Diet.*, 2014, **3**, 147–156.
27 G. Ekanayake, S. Wijayawardana, M. Jayanetti, C. Thambiliyagodage, H. Liyanaarachchi and A. Mendis, *Sci. Rep.*, 2025, **15**, 35743.
28 R. Vehring, *Pharm. Res.*, 2008, **25**, 999–1022.
29 S. Y. Quek, N. K. Chok and P. Swedlund, *Chem. Eng. Process.*, 2007, **46**, 386–392.
30 T. C. Kha, M. H. Nguyen and P. D. Roach, *J. Food Eng.*, 2010, **98**, 385–392.
31 R. V. Devakate, V. V. Patil, S. S. Waje and B. N. Thorat, *Sep. Purif. Technol.*, 2009, **64**, 259–264.
32 K. Samborska, D. Witrowa-Rajchert and A. Gonçalves, *Drying Technol.*, 2005, **23**, 941–953.
33 S. Rocha, R. Generalov, C. Pereira Mdo, I. Peres, P. Juzenas and M. A. Coelho, *Nanomedicine*, 2011, **6**, 79–87.
34 T. H. Do, T. C. Kha and P. P. T. Huynh, *J. Agric. Dev.*, 2019, **18**, 49–57.
35 F. Zhu, B. Du and B. Xu, *Food Hydrocoll.*, 2016, **52**, 275–288.
36 E. M. Both, R. M. Boom and M. A. I. Schutyser, *Powder Technol.*, 2020, **363**, 519–524.
37 D. E. Walton, *Drying Technol.*, 2000, **18**, 1943–1986.
38 Z. Réblová, *Czech J. Food Sci.*, 2012, **30**, 171–175.
39 J. Wang, H. Li, Z. Chen, W. Liu and H. Chen, *Ind. Crop. Prod.*, 2016, **89**, 152–156.
40 A. Munin and F. Edwards-Lévy, *Pharmaceutics*, 2011, **3**, 793–829.
41 A. Ali Redha, C. Kodikara and D. Cozzolino, *Nutrients*, 2024, **16**, 3625.
42 M. Cheng, X. Yan, Y. Cui, M. Han, Y. Wang, J. Wang, R. Zhang and X. Wang, *Polymers*, 2022, **14**, 1214.
43 P. Pasukamonset, O. Kwon and S. Adisakwattana, *Food Hydrocoll.*, 2016, **61**, 772–779.
44 A. Gharsallaoui, G. Roudaut, O. Chambin, A. Voilley and R. Saurel, *Food Res. Int.*, 2007, **40**, 1107–1121.
45 C.-H. Tang and C.-Y. Ma, *Food Chem.*, 2009, **115**, 859–866.
46 V. Valková, H. Ďúranová, A. Falcimaigne-Cordin, C. Rossi, F. Nadaud, A. Nesterenko, M. Moncada, M. Orel, E. Ivanišová, Z. Chlebová, L. Gabríny and M. Kačániová, *Foods*, 2022, **11**, 2267.
47 M. L. Y. Wan, V. A. Co and H. El-Nezami, *Crit. Rev. Food Sci. Nutr.*, 2021, **61**, 690–711.
48 J. A. Zokti, B. Sham Baharin, A. S. Mohammed and F. Abas, *Molecules*, 2016, **21**, 940.
49 J. O. Airouyuwa, P. Mudgil and S. Maqsood, *Food Sci. Nutr.*, 2025, **13**, e70535.
50 Ö. A. Gümüşay, İ. Cerit and O. Demirkol, *Foods*, 2025, **14**, 625.
51 F. Ahmadi, H. A. R. Suleria and F. R. Dunshea, *Foods*, 2025, **14**, 237.